Proceedings of The National Conference
On Undergraduate Research (NCUR) 2019
Kennesaw State University
Kennesaw Georgia
April 10 – 13, 2019

Thermal Analysis of the Specific Heat of $Pr_{1-x}Nd_xOs_4Sb_{12}$

Yeh-Chia Chang[1], Shoji Hishida[1], Jesus Velasquez[1], Taylor McCullough-Hunter[1], Pei-Chun Ho[1], M. Brian Maple[2], Tatsuya Yanagisawa[3]
[1]Department of Physics
California State University
Fresno, CA 93740, USA

[2]Department of Physics
University of California, San Diego
La Jolla, CA 92093, USA

[3]Department of Physics
Hokkaido University
Sapporo, Hokkaido 060-0808, Japan

Faculty Advisor: Dr. Pei-Chun Ho

Abstract

The specific heat of single-crystal clusters of the filled-skutterudite compound $Pr_{1-x}Nd_xOs_4Sb_{12}$ were measured in the temperature range from 11K to 300 K for samples with different Nd concentrations, x. A curve fit of the molar specific heat as a function of temperature was evaluated for each sample in order to determine contributions to the specific heat from the atoms of the lattice and from the conduction electrons. A combination of the Debye and Einstein models of heat capacity were applied to account for the lattice contributions, while the Sommerfeld model was applied for the conduction electron contribution. This allows for the estimation of thermodynamic parameters such as the Debye temperature, Einstein temperature, the electronic specific heat coefficient, and a weighting factor that determines the relative contributions from the Debye model and the Einstein model to the density of states. The evolution of the parameters with respect to Nd concentration can then be determined.

Keywords: Filled Skutterudites, Specific Heat, Relaxation Calorimetry

1. Introduction

The Filled Skutterudites include materials that have the chemical formula RT_4X_{12} where R is a rare-earth metal, T is a transition metal, and X is a pnictogen. In our case, the rare-earth metals under consideration are Praseodymium (Pr) and Neodymium (Nd), the transition metal is osmium (Os), and the pnictogen is Antimony (Sb). There is interest in studying these materials due to their interesting properties at low temperatures. $PrOs_4Sb_{12}$ has been found to exhibit unconventional heavy-fermion superconductivity with a transition temperature of $T_c \approx 1.85$ K,[1] and $NdOs_4Sb_{12}$ becomes ferromagnetic below $T_{Curie} \approx 0.9$ K.[1, 2] By studying the intermediate compounds of $Pr_{1-x}Nd_xOs_4Sb_{12}$, the interplay between the superconducting and magnetic effects can be examined.

Figure 1 shows the low-temperature phase diagram of $Pr_{1-x}Nd_xOs_4Sb_{12}$ with respect to the Nd concentration, x. This phase diagram was obtained from previous work and takes into consideration the results of a variety of different measurements, including AC magnetic susceptibility, resistivity, specific heat, and muon spin relaxation (μSR).[1, 3]

The superconducting transition temperature (T_c) and the Curie temperature (T_{Curie}) become suppressed towards the intermediate range of x, and of particular interest is the range $0.40 \leq x \leq 0.55$ where the superconductivity and ferromagnetism were found to coexist in the samples at low temperatures.[1] At the Nd concentration x ~0.55 where the superconductivity disappears, either a quantum phase transition (QPT) or quantum critical point (QCP) may exist.

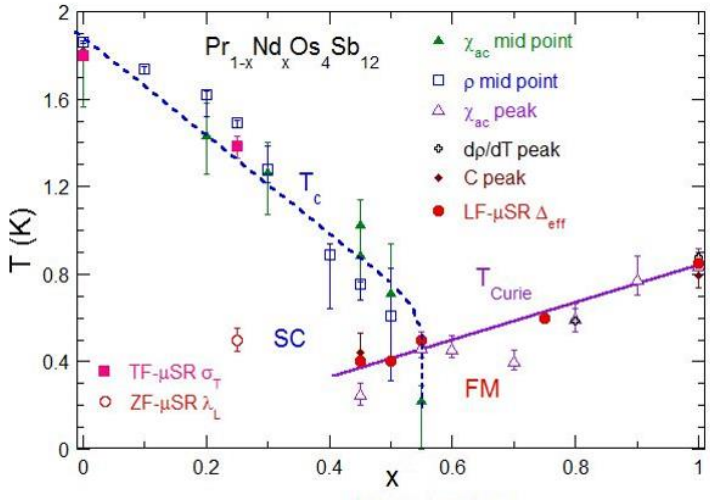

Figure 1: Superconducting transition temperature (T_c) and Curie temperature (T_{Curie}) as a function of Nd concentration (x) in $Pr_{1-x}Nd_xOs_4Sb_{12}$. [1]

In order to better understand the behavior of this system of materials, it is also necessary to characterize the sample properties for temperatures above these transition temperatures (i.e., normal state property). The filled skutterudite structure is known for its rattling effect. $Pr_{1-x}Nd_xOs_4Sb_{12}$ is the doping system which represents the trade-off between superconductivity and magnetism. While the rattling effect is involved in the phonons movement, multiband superconductivity[4] in this system could be influenced by the traditional electron-phonon mechanism. Therefore, the phonon state of the sample should be explored further. Debye and Einstein temperature are two parameters relative to phonons and both are important to acknowledge normal state properties of the materials. In this paper, we report on measurements of the specific heat for clusters of single crystals of $Pr_{1-x}Nd_xOs_4Sb_{12}$ in the temperature range from ~11 – 300 K. The temperature-dependence of the specific heat can provide information about the vibrational properties of the lattice structure as well as correlation of the electrons.

2. Experimental Set-Up

The single-crystal samples of $Pr_{1-x}Nd_xOs_4Sb_{12}$ presented here were grown by our group members at the sample-preparation facility at Prof. Brian Maple research laboratory at University of California, San Diego, and were synthesized using an antimony self-flux method.[5] The rare-earth starting materials (Nd and Pr) were combined in an arc-melting furnace, then the rare-earths and the other starting materials (Os and Sb) were combined with an excess of antimony, sealed within a carbon-coated quartz tube, and subjected to a heating cycle in a box furnace. The single crystals were then separated from the excess antimony first by flux spinning at 700°C, then by chemical etching.

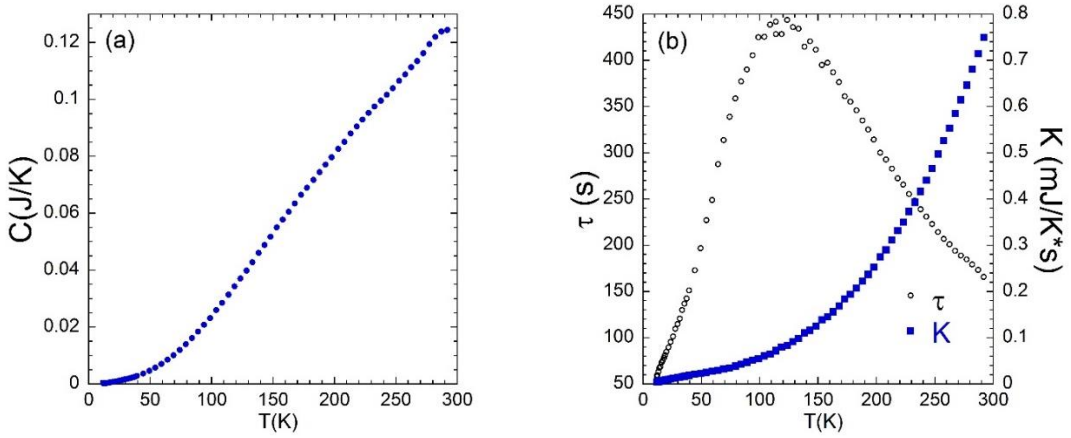

Figure 2: (a) Heat capacity (C) of the empty calorimeter versus temperature (T). (b) The time constant τ and thermal conductance K between the empty calorimeter to cold finger of the cryocooler as a function of T.

The heat capacity of single-crystal clusters of $Pr_{1-x}Nd_xOs_4Sb_{12}$ was measured using a laboratory-built relaxation calorimeter.[6] The masses of the crystal samples measured typically fell in the range from 100 – 200 mg, along with 1 - 4 mg of Apiezon N-Grease used to mount the sample to the calorimeter platform. The calorimeter probe was placed inside of an APD Cryogenics cryocooler system, which can be cooled under vacuum from room temperature down to temperatures of ~ 10 K. The temperature of the calorimeter was measured using a Cernox™ bare-chip resistance thermometer from LakeShore Cryotronics and the heater for the calorimeter consisted of a 2 kΩ resistor.

There are two graphs in Fig. 2 showing the information of the empty calorimeter. Figure. 2(a) is the heat capacity of calorimeter itself as a function of the temperature (T), while Fig. 2(b) displays the T-dependence of thermal relaxation time constant (τ) and thermal conductance (K) between the calorimeter to cold finger of the cryocooler. The time constant τ had a maximum up to 450 seconds when the temperature was approximately 120K. The thermal conductance K grew up to 0.8 mJ/K-s with increasing temperature.

Figure 3(a) displays the raw data of a heat-capacity measurement at temperature baseline T_0 (~279.4 K). The red square line is the heat pulse that the heater supplied to the substrate and sample. The pulse width (t_w) was equal to t_f - t_i, which was 240 seconds for all the measurements. The time t_i and t_f is the initial and final time when we turn on and off the heat. The blue data curve is the temperature trace of a real experimental data set for T_{mid}, which is defined as $T_0+\Delta T_{meas}/2$. If the heat pulse is longer than eight times τ, the sample and background will reach the thermal equilibrium, like the gray dashed line in the graph, and have a temperature difference of ΔT_{eq} compared to T_0. However, in order to increase the rate of taking data, a shorter pulse width in the measurement was shut down before the thermal equilibrium, when the temperature change ΔT_{meas} was reached. For accuracy, the value of the $\Delta T_{meas}/T_0$ was controlled in a certain range, 1%-2% differing with temperature by adjusting the power.

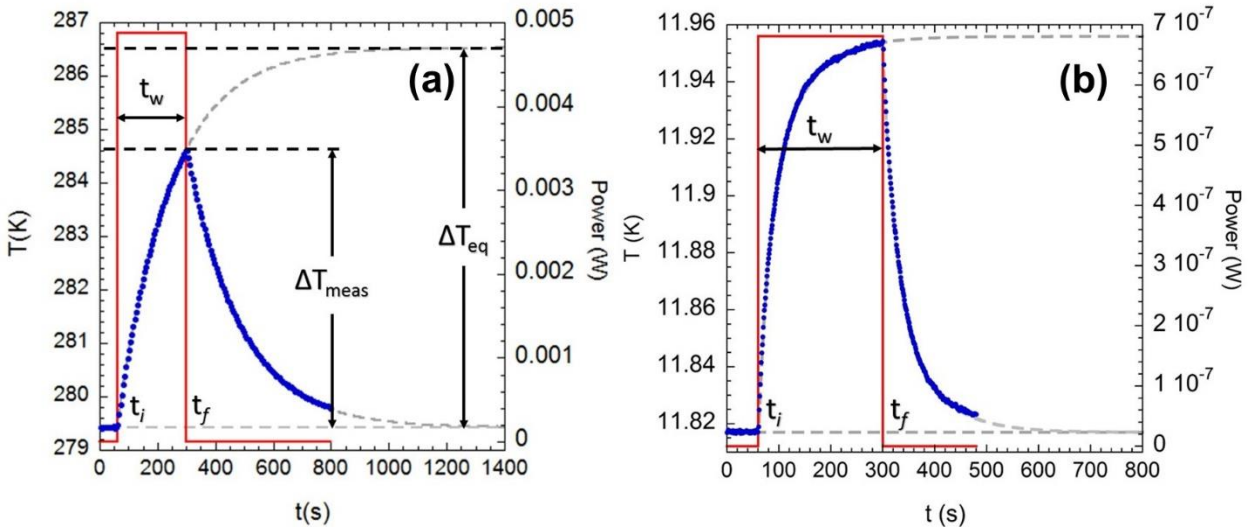

Figure 3: (a) Temperature (T) vs time (t) of the relaxation calorimeter (blue solid circles), which shows a 1-τ behavior. The red line is the heat pulse applied during the heat capacity measurement. (b) Raw data of T(t) shows a 2-τ behavior with applied power.

The 2-τ model[7] would be applied to extract the heat capacity when the thermal contact between the substance and the sample becomes finite. Figure 3(b) shows the raw data of 2-τ when we were measuring the background with the grease. In the experiment, 2-τ appeared at lower temperature most likely and ranged from 11K to 45K. The 2-τ model only showed when we measured the background or with the grease. Once we measured the heat capacity with crystals, the 1-τ model is sufficient to determine the heat capacity data.

3. Experimental Results and Data Analysis

The heat capacity of samples of $Pr_{1-x}Nd_xOs_4Sb_{12}$ was measured for Nd concentrations of x = 0.10 to x = 1.00 over the temperature range from ~11 – 300 K. The temperature increment was 1K at 11K – 20K, 2K at 22 – 40K, and 5K above 45K. To lower the error for the x= 0.5 sample from 100K to 150K, the increment was set to 2.5K. The measured specific heat of samples is shown in Fig. 4 and each of the data sets follow a similar trend, with specific heat values approaching the predicted value 51R from the Dulong-Petit Law at higher temperatures where R is the universal gas constant 8.314 J/(mol·K). The challenging for the project is the noisy data at the high temperature.

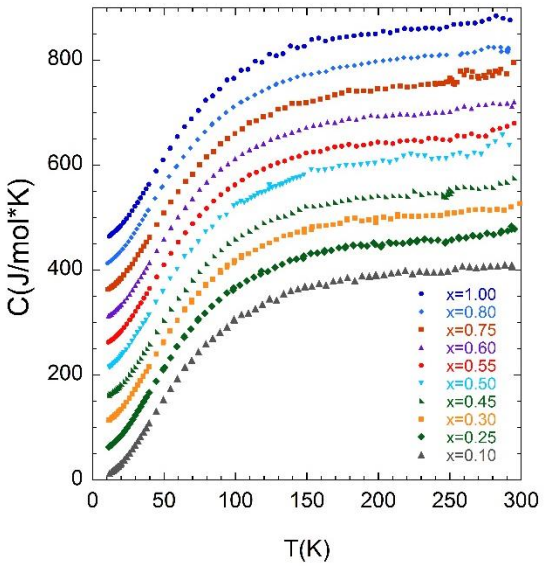

Figure 4: Molar specific heat of $Pr_{1-x}Nd_xOs_4Sb_{12}$ over the temperature range from ~ 11 – 300 K. For easier visual comparison, each data set is offset by increments of 50 J/(mol·K).

The specific heat for a given material includes both contributions from the conduction electrons and from the lattice vibration of atoms. In order to analyze the specific heat as a function of temperature for our samples, we applied a combination of models to account for these contributions.

For the electronic contribution to specific heat the Sommerfeld model[8] was applied, with the assumption that the Fermi temperature is very large compared to the temperatures being measured. This model predicts an electronic specific heat of the form:

$$c_{\text{el}} = \gamma T \qquad (1)$$

where γ is the electronic specific heat coefficient.

Phonons[9] are particles used to describe the lattice vibrations in a solid. As external heat or force is applied on a lattice, it generates vibrations that can be represented as the movement of phonons through the material. A phonon is the quantized particle of the collective vibrations in quantum mechanics. Thus, phonons play an important role in the thermal and electrical properties of a given compound. In the phonon dispersion relation, there are typically two modes: one is the optical mode, which occurs at higher frequencies and the other is the acoustic mode, which occupies the lower frequency regime.

For the lattice specific heat, the Debye and Einstein models of specific heat were used in conjunction to describe the overall lattice specific heat. The reason for the inclusion of both models is the presence of a rattling mode that takes place in these materials, as suggested by previous observations of peaks in the ultrasonic attenuation coefficient at low temperatures.[10, 11] In the crystal structure of the filled-skutterudites, the pnictogen atoms form a cage-like structure around the rare-Earth atom, and the rare-Earth oscillates within this structure.[10, 11] The rattling mode is better approximated by the Einstein Model of specific heat, which treats the atoms of the lattice as independent oscillators oscillating at a single frequency, referred to as the Einstein frequency (ω_E). The Debye Model considers the lattice as an oscillating continuum up to a cut-off frequency referred to as the Debye frequency (ω_D), and this model is used to account for the specific heat behavior of the majority of the atoms that make up the lattice. The dispersion relations and the density of states (DOS) for the Debye and Einstein Models are given in Fig. 5(a) and 5(b). The DOS(ω) as a function of frequency (ω) is the number of modes per unit frequency range and the total mode can be described by $\int \text{DOS}(\omega)d\omega$. Debye model predicts a linear dispersion relation and a quadratic DOS up to the ω_D, while the Einstein model predicts a flat line dispersion relation and a delta function at ω_E for DOS.

For most of the metallic compounds, ω_E is associated with optical modes and has a much higher frequency than ω_D, which is associated with the acoustic modes. However, for the filled skutterudite compounds, the ratting effect of rare

earth ions can cause a large increase of phonon density at certain frequency below ω_D. Therefore, the Einstein mode is used in addition to the Debye model to simulate this anomaly in the fitting of specific heat data of $Pr_{1-x}Nd_xOs_4Sb_{12}$.

The formulas for the lattice contribution to the molar specific heat per unit formula ROs_4Sb_{12} have the following form:

$$c_{\text{Lattice}} = (17 - r)c_{\text{Debye}} + rc_{\text{Einstein}} \tag{2}$$

$$c_{\text{Debye}} = 9R\left(\frac{T}{\theta_D}\right)^3 \int_0^{\theta_D/T} \frac{x^4 \exp(x)}{(\exp(x)-1)^2} dx \tag{3}$$

$$c_{\text{Einstein}} = 3R\left(\frac{\theta_E}{T}\right)^2 \frac{\exp(\theta_E/T)}{(\exp(\theta_E/T)-1)^2} \tag{4}$$

where r is a weighting factor for the Einstein mode, θ_D is the Debye Temperature, θ_E is the Einstein Temperature, and R is the universal gas constant. θ_D has the relation with ω_D as $\theta_D = \hbar\omega_D/k$ while θ_E has the same relation with ω_E as $\theta_E = \hbar\omega_E/k$. The total contribution for the specific heat is 17 lattice, which came from the number of the atoms in the chemical formula RT_4X_{12} of filled skutterudites. The symbol r is a weighting factor that determines the relative contributions of the two models.

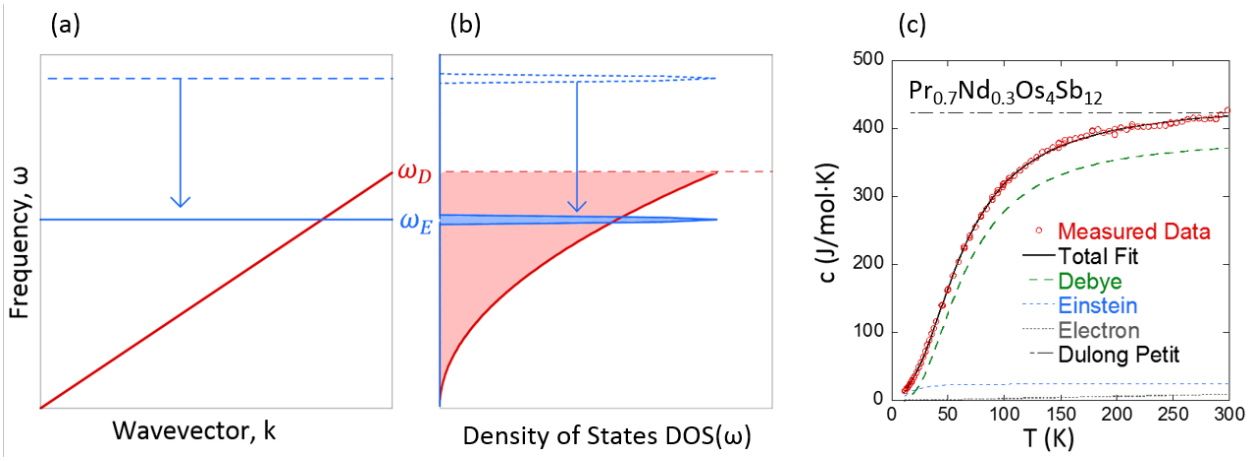

Figure 5: (a) Dispersion relation associated with the Debye and Einstein Models. (b) The density of states for the Debye and Einstein models. (c) An example of the curve-fitting of the specific heat of the measured data for the x = 0.30 sample.

The plot shows the breakdown of the fit into contributions from the Debye Model, Einstein Model, and Electronic specific heat, and compares these values with the high-temperature limit predicted by the Dulong-Petit Law.

The models of specific heat $c(T) = c_{\text{el}} + c_{\text{Lattice}}$ were applied to the measured specific heat vs. temperature data and a curve fit was implemented using MATLAB in order to determine values for parameters including the Debye Temperature (θ_D), the Einstein Temperature (θ_E), the weighting factor (r) and the electronic specific heat coefficient (γ). An example of the curve-fit output for the x = 0.30 sample is shown in Fig. 5(c).

The Debye temperature provides a measure of the lattice stiffness, while the Einstein temperature is associated with the rattling mode of the rare-earth ion. The ratio of r/(17- r) determines the relative magnitude of the contributions to the DOS from Einstein to Debye models. The value of the electronic specific heat coefficient γ provides information about how strongly the electrons are correlated with each other.

Figure 6 depicts (a) Debye Temperature, (b) Einstein Temperature, (c) the weighting factor r and (c) the electronic specific heat coefficient γ as a function of x, respectively. Table 1 lists reduced chi-square (no weighting) and adjusted R-square for each Nd concentration to indicate the goodness of the fit. All parameters seemed to have a minimum when x is in the middle around x=0.45-0.50. The value of the parameters increase with x going towards either of the end-member compounds. However, for each of the parameters, there are some data points that jump or drop unexpectedly and do not fit the trends in the rest of the data. The Debye and Einstein temperatures produced from x=0.45 and 0.75 had higher values than expected. For the weighting factor, the parameter estimate for x = 0.75 had a larger error bar. The estimates for the electronic specific heat coefficient had relatively low error values, but there was a bump for x ~ 0.50 in the middle of the 'v' character for other points. Nevertheless, the overall minimum region in x strikingly closes to the neodymium concentration where superconductivity disappears. Since θ_D and θ_E also have a dip in this region, phonons seem to become softening here. In order to determine whether this effect has a correlation with the suppression of superconductivity near a QPT or QCP, further study such as experiments of ultrasound or pressure will be required.

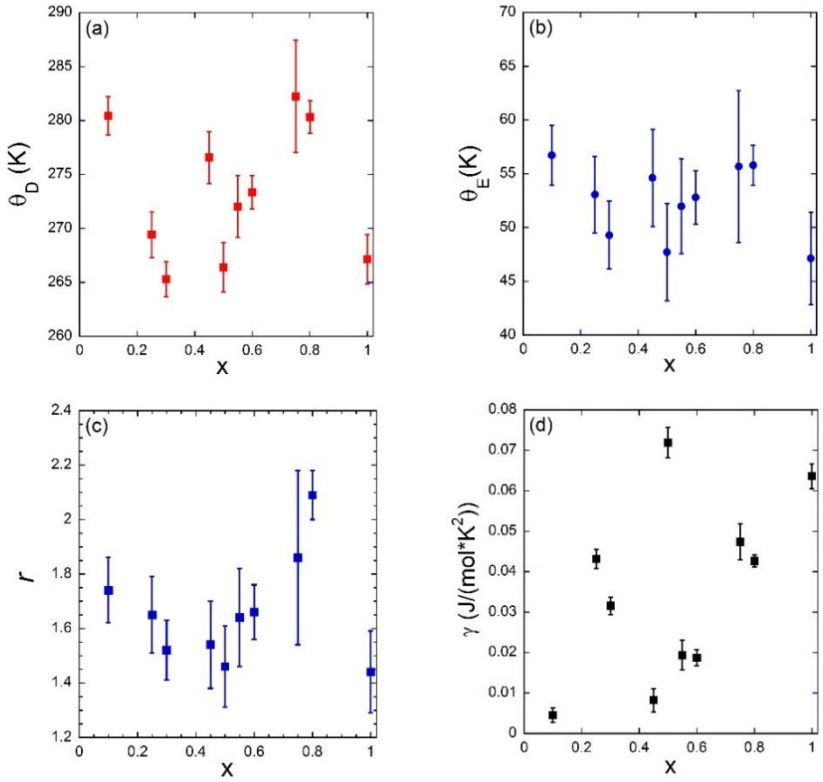

Figure 6: Extracted values of curve-fitting parameters for different concentrations of Nd (x) within the sample. The fitting parameter are (a) the Debye temperature, (b) the Einstein temperature, (c) the weighting factor r, and (d) the electronic specific heat coefficient.

Table 1. Reduced Chi-Square (no weighting) and adjusted R-square of curve-fitting of specific heat with different concentrations of Nd (x).

x	0.10	0.25	0.30	0.45	0.50	0.55	0.60	0.75	0.80	1.00
Reduced Chi-Sqr	7.0495	10.8456	7.4687	15.1476	12.3163	20.9442	6.1092	51.6205	4.569	10.9919
Adj. R-Sqr	0.99992	0.99989	0.99992	0.99983	0.99987	0.99976	0.99993	0.99953	0.99995	0.99988

4. Conclusion

The molar specific heat of single-crystal clusters of $Pr_{1-x}Nd_xOs_4Sb_{12}$ was measured over the temperature range from 11K to 300K for samples with varying Nd concentrations. The specific heat was analyzed by combining the Debye, Einstein, and Sommerfeld models to fit the measured data. Material parameters, such as the Debye temperature, Einstein temperature, weighting factor, and electronic specific heat coefficient, were extracted through the curve fitting. The trends of these parameters with respect to sample composition represent the properties of this doping system. In the current state, minima can be found near $x \sim 0.50$ for Debye temperature, Einstein temperature, the weighting factor, and electronic specific heat coefficient. Although all four parameters exhibit large errors that make it difficult to specify the precise trend with respect to x, the trend showing the minima can still be observed on the whole. Therefore, further work needs to be done to improve the curve fitting and analysis to resolve the trends in these parameters. This work may include re-measuring samples with outlier data and checking the curve-fitting program to verify that the algorithm is converging to a global rather than local minimum.

5. Acknowledgements

Research at CSU-Fresno is supported by NSF DMR-1506677; at UCSD by NSF DMR-1810310 and US DOE DEFG02-04ER46105; at Hokkaido Univ. by JSPS KAKENHI grants nos. 26400342, 15K05882, and 15K21732.

6. References

1. D.E. MacLaughlin, P.-C. Ho, L. Shu, O.O. Bernal, S. Zhao, A.A. Dooraghi, T. Yanagisawa, M.B. Maple, R.H. Fukuda. “Muon spin rotation and relaxation in Pr1-xNdxOs4Sb12: Magnetic and superconducting ground states.” *Physical Review B.* **89**, 144419 (2014)

2. P.-C. Ho, W. M. Yuhasz, N. P. Butch, N. A. Frederick, T. A. Sayles, J. R. Jeffries, M. B. Maple, J. B. Betts, A. H. Lacerda, P. Rogl, and G. Giester. “Ferromagnetism and possible heavy fermion behavior in single crystals of NdOs4Sb12 ,” *Physical Review B* **72**, 094410 (2005).

3. P.-C. Ho, T. Yanagisawa, W. M. Yuhasz, A. A. Dooraghi, C. C. Robinson, N. P. Butch, R. E. Baumbach, and M. B. Maple. “Superconductivity, magnetic order, and quadrupolar order in the filled skutterudite system Pr1-xNdxOs4Sb12.” *Physical Review B*. **83**, 024511 (2011)

4. G. Seyfarth, J.P. Brison, M.-A. Méasson, J Flouquet, K. Izawa, Y. Matsuda, H. Sugawara, and H. Sato. *Phys. Rev. Lett.* **95** 107004 (2005)

5. E.D. Bauer, A. Slebarski, E.J. Freeman, C. Sirvent, M.B. Maple. “Kondo insulating behavior in the filled skutterudite compound CeOs4Sb12.” *Journal of Physics: Condensed Matter*. **13**, 4495-4503 (2001)

6. H.A. Anderson, U.L. Urbina, P.-C. Ho. “Constructing a relaxation calorimeter.” *Proceedings of the National Conference on Undergraduate Research (NCUR) 2013.* University of Winsonsin La Crosse, WI (2013)

7. J.P. Shepherd. “Analysis of the lumped τ2 effect in relaxation calorimetry.” *Review of Scientific Instruments*. **56**. 273 - 277. 10.1063/1.1138343. (1984)

8. C. Kittel. (1996). *Introduction to Solid State Physics*. 7th ed. New York: Wiley, p. 155. (1996)

9. C. Kittel. (1996). Phonon I. Crystal Vibration. *Introduction to Solid State Physics* 7th ed. New York: Wiley, p.99-114. (1996)

10. Y. Nemoto, T. Ueno, N. Takeda, T. Yamaguchi, T. Yanagisawa, T. Goto, H. H. Sugawara, H. Sato. “Ultrasonic dispersion and off-center rattling in heavy fermion superconductor PrOs4Sb12.” *Physica B*, **370-380**, p. 184-186 (2006)

11. T. Yanagisawa, P.-C. Ho, W.M. Yuhasz, M.B. Maple, Y. Yasumoto, H. Watanabe, Y. Nemoto, T. Goto. “Ultrasonic investigation of off-center rattling in filled skutterudite compound NdOs4Sb12.” *Journal of the Physical Society of Japan*. **Vol. 77**, No. 7, 074607 (2008)